Science Advances

AAAS

advances.sciencemag.org/cgi/content/full/4/1/eaap9722/DC1

# Supplementary Materials for

## Toward biomass-derived renewable plastics: Production of 2,5-furandicarboxylic acid from fructose

Ali Hussain Motagamwala, Wangyun Won, Canan Sener, David Martin Alonso, Christos T. Maravelias, James A. Dumesic

Published 19 January 2018, *Sci. Adv.* **4**, eaap9722 (2018)
DOI: 10.1126/sciadv.aap9722

**This PDF file includes:**


- Supplementary Materials and Methods
- fig. S1. Chromatogram of product solution obtained by the dehydration of fructose.
- fig. S2. CO chemisorption isotherms for the 5% Pt/C catalyst.
- fig. S3. Image showing the separation of catalyst, solvent, and crystallized FDCA.
- fig. S4. PDA chromatogram of freeze-dried FDCA.
- fig. S5. Gas chromtography–mass spectrometry analysis of freeze-dried FDCA.
- fig. S6. Nuclear magnetic resonance spectroscopy analysis of freeze-dried FDCA.
- fig. S7. Differential scanning calorimetry curve of freeze-dried FDCA.
- fig. S8. Process block flow diagram for the integrated FDCA production strategy.
- fig. S9. Safety in the oxidation reactor.
- table S1. Product composition after fructose dehydration using FDCA as a dehydration catalyst.
- table S2. Product concentration before and after removal of humins by adsorption.
- table S3. Characterization of the Pt/C catalyst.
- table S4. Results for HMF oxidation reactions over the 5% Pt/C catalyst (under 40-bar $O_2$ pressure and 383 K).
- table S5. Mass and energy balances (basis: 500 metric tons of fructose per day).
- table S6. Energy requirements (basis: 500 tons of fructose per day).
- table S7. Capital and operating costs (basis: 500 metric tons of fructose per day).
- table S8. List of economic parameters and assumptions.
- table S9. Effect of transport resistance and $O_2$ pressure on HMF oxidation over a Pt/C catalyst.
- References (*29*–*34*)

## Supplementary Materials and Methods

### Oxidation of fructose-derived HMF

Solution obtained after fructose dehydration with HCl as the acid catalyst was oxidized as described in the main text. Oxidation of this HMF solution resulted in low FDCA yield due to catalyst deactivation (Table 1, entry 4). We determined that there are two separate effects that lead to catalyst deactivation. Oxidation of commercial HMF containing small amounts of HCl (equivalent to the amount used in our fructose dehydration experiments) reaction led to poor FDCA yield (table S4, entry 1). Comparison of the results of HMF oxidation with and without the presence of $Cl^-$ ion (Table 1, entry 3 and table S4, entry 1) demonstrates that the $Cl^-$ ion deactivates the Pt/C catalyst. For this reason, we used an ion exchange resin (Amberlite IRA-400) to remove the chloride ion from the HMF obtained from fructose dehydration. When this $Cl^-$ free HMF feed obtained after ion exchange was oxidized over Pt/C catalyst, however, a poor yield of FDCA (~18%) was obtained (table S4, entry 2), suggesting that the humins produced during dehydration of fructose are another cause for catalyst deactivation. Accordingly, we subsequently removed these humins by adsorption over activated carbon, while retaining >95% of the HMF produced during fructose dehydration. Treatment of HMF produced from fructose dehydration by ion exchange to remove $Cl^-$ ions and by contacting with activated carbon to remove humins produced a liquid stream of GVL/$H_2O$ containing HMF that could be oxidized over Pt/C to FDCA in 93% FDCA yield (Table 1, entry 5).

### Pt/C catalyst stability

A stability test of the Pt/C catalyst was carried out in a fixed bed reactor operating in an up-flow configuration. The catalyst was placed in a stainless steel tubular reactor (12.7 mm OD) and held between two end plugs of silica granules and quartz wool. The feed was introduced into the reactor using an HPLC pump (Lab Alliance Series I). Simulated feeds for catalytic experiments were prepared by adding commercial HMF to the GVL:$H_2O$ (50:50) solution. The flow of $O_2$ during the reaction (25 ml (STP)/min) was controlled by a mass flow controller (Brooks Instruments, 5850S). The tubular reactor was fitted inside an aluminum block and placed within an insulated furnace. Bed temperature was monitored at the reactor wall using a Type K thermocouple (Omega) and controlled using a 16A series programmable temperature controller (Love Controls). Reactor pressure (35 bar of $O_2$) was controlled using a back pressure regulator. The reactor effluent flowed into a vapor-liquid separator wherein the liquid product was collected periodically. The liquid sample was analyzed as described before.

### FDCA crystallization

FDCA crystalized during the cooling of reactor from reaction temperature to 303 K, and it was separated from the solid catalyst by the following procedure. The solvent was first separated from solid catalyst and crystalized FDCA by centrifugal filtration using a centrifuge tube equipped with a 0.2 μm PTFE Filter (ChromTech™). The filtrate was heated to 373 K in a thick glass tube (Alltech®) and hot solvent was passed through the solid mixture to dissolve the FDCA at elevated temperature and leave behind the insoluble catalyst. The filtrate after separation from catalyst was cooled to 277 K where FDCA crystalized. Figure S3 shows pictorially a typical catalyst separation and FDCA crystallization. FDCA crystals were separated

from the GVL/$H_2O$ solution by decantation, and were washed with cold Milli-Q water to remove GVL and were freeze dried to obtain dry solid FDCA.

**FDCA purity**

The purity of dried FDCA obtained after separation and crystallization was determined by the following four techniques:

**1. HPLC:**

5 mg of dried FDCA was dissolved in 1.5 ml of 0.05M NaOH solution. The above solution was analyzed by HPLC using a Bio-Rad Aminex HPX-87H column on a Waters 2695 system equipped with PDA-2998 detector. The temperature of the HPLC column was maintained at 338 K, and the flow rate of the mobile phase (pH=2 water, acidified by sulfuric acid) was 0.6 ml/min. Figure S4 shows the PDA chromatogram of dried FDCA.

**2. GC-MS:**

2 mg of dried FDCA was added to a mixture of 0.9 ml of dichoromethane, 0.1 ml of pyridine and 0.1 ml of N,O-Bis(trimethylsilyl)trifluoroacetamide (BSTFA). The above mixture was kept in a sand bath at 323 K for 1 hour to silylate FDCA. After derivatization, the sample was analyzed by gas chromatography/mass spectrometry (GC/MS) (Shimadzu GCMS-QP2010S equipped with a SHRXI-5MS capillary column). The GC-MS chromatogram of the product is shown in fig. S5, in which no peaks from impurities can be observed.

**3. $^{1}$H and $^{13}$C NMR**

$^{1}$H and $^{13}$C NMR spectroscopy was performed on a Bruker 400 MHz NMR spectrometer. 10 mg of dried FDCA was dissolved in 1.5 ml of deuterated DMSO. NMR spectra were referenced against tetramethylsilane (TMS). Figure S6 shows the $^{1}$H and $^{13}$C spectra of dried FDCA. The purity of the sample was determined to be >99% from the $^{1}$H spectra.

**4. Differential Scanning Calorimetry (DSC)**

Differential scanning calorimetry (DSC) experiments were carried out on a DSC Q100 differential calorimeter (TA Instruments) equipped with an autosampler and mass flow control. The 1.6 mg of dried FDCA was placed in hermetically closed DSC capsule. The DSC capsules were equilibrated at 303 K, heated to 643 K at 10 K/min, equilibrated at 643 K, and cooled to 303 K at 10 K/min. The DSC curve showing the heat flux with respect to the temperature is shown in fig. S7. The melting temperature of FDCA was determined to be 605 K.

**Techno-economic analysis**

To demonstrate techno-economic feasibility of the process, we calculated the minimum selling price (MSP) of FDCA produced using the proposed strategy. Our techno-economic analysis follows the following four steps.

The first step is the design of the process that is divided into seven sections as shown in fig. S8. Models for the HMF production section, FDCA production section, FDCA separation section, and solvent separation section were developed in Aspen Plus (V8.8 Aspen Technology) based on the experimental data, while the other sections (wastewater treatment, storage, and utilities) were scaled based on the NREL model (*29*). In HMF production section, fructose is converted to

HMF, Levulinic acid (LA), and furfural in 70.0%, 8.7%, and 3.4% molar yields, respectively. It is assumed that the remaining fructose is degraded to humins. Following the fructose conversion reaction, humins are separated by adsorption on activated carbon. During regeneration of the adsorption bed using oxygen, a part of humins (57.2 wt% carbon in humins) is converted to activated carbon which could be sold as a byproduct. In FDCA production section, HMF is oxidized to FDCA in 93% molar yield over 5 wt% Pt/C catalyst and in the FDCA separation section, solvent-dissolved FDCA is cooled to 298 K. This decrease in temperature causes FDCA to precipitate and enables us to efficiently recover FDCA using solid-liquid separators. In solvent separation section, excess water generated during fructose dehydration is separated by distillation and the GVL stream, containing LA is sent over to a reactor containing $RuSn_4$/C catalyst. In this reactor, LA is upgraded to GVL to make up for the loss of GVL. The mass and energy balances for the main streams are presented in table S5.

The second step is the heat integration to optimize energy use using Aspen Energy Analyzer (V8.8 Aspen Technology). Our process has heating requirements (41.1 MW) mainly due to the evaporation of water and separation of GVL for recycling (30.4 MW). After heat integration, we obtained significant energy recovery (34.2 MW), thereby reducing the heating requirements of the process to 6.9 MW (table S6). The cooling and electricity requirements of the process are estimated to be 22.0 MW and 0.3 MW, respectively. The heating, cooling and electricity requirements after heat integration are satisfied by external sources.

The third step is the equipment sizing and cost analysis. A part of the equipment cost in HMF production, FDCA production, FDCA separation, and solvent separation sections was estimated using Aspen Process Economic Analyzer (V8.8 Aspen Technology). The equipment cost of the remaining sections was estimated using a scaling expression based on the equipment size and cost data in NREL report (*29*). All equipment and material costs were adjusted to a common basis year of 2015. Table S7 shows the capital and operating costs for all processing sections. The total capital investment is estimated to be $83.3 million. The total operating cost is $124.4 million/year.

The fourth step is the calculation of the MSP of FDCA following the NREL approach (using a discounted cash flow analysis (*29*) and economic parameters and assumptions (table S8)) based on the capital and operating costs. The MSP of FDCA is estimated to be $1490 per ton of FDCA.

**Effect of transport resistance and oxygen pressure on HMF oxidation**

Catalyst stability studies were performed in a flow-through fixed bed reactor wherein the Pt/C catalyst bed was held between two end-plugs of silica granules and quartz wool. The liquid feed containing HMF was introduced into the reactor using an HPLC pump at a desired flow rate. Simultaneously, oxygen gas was flowed at the desired flow rate leading to a three phase reaction system. We studied this system for transport resistances by varying the flow rate while keeping the space velocity constant, by changing the catalyst volume in the reactor (table S9). From table S9, it is observed that the yield of FDCA and FFCA remained constant while the liquid and gas flow rates were changed, indicating that there are negligible external transport resistances present.

The effect of oxygen pressure was also studied. As shown in table S9, the yield of FDCA and FFCA remained constant by changing the oxygen pressure from 40 bar to 20 bar, indicating that the reaction is insensitive to oxygen pressure. Recent work by Davis et al., investigating HMF oxidation over Pt, also reports a zero order dependence on oxygen pressure (*30*).

**Safety consideration for aerobic oxidation**

The combination of molecular oxygen and an organic solvent can represent a significant safety concern. Mixture of $O_2$ and the vapors of the solvent system (GVL:$H_2O$ (50:50)) can create a flammable atmosphere; thus the reaction condition must be carefully selected to ensure safe operation.

Solvent vapor and oxygen mixture is capable of combustion if sufficient heat (ignition source), fuel (organic vapor), and oxidizer (oxygen) are present. Combustion can be prevented if anyone of the above three elements is removed. However, under reaction condition it is difficult to reliably remove the ignition sources, thus one of the most practical approach towards a safe operation is to conduct the reaction below the lower flammability limit (LFL) of the organic solvent used in the reaction. Under this condition there is not enough fuel to sustain combustion. Generally, LFL decreases with an increase in temperature. Figure S9 shows lower flammability limit of GVL as a function of temperature. The pressure at which the vapor pressure of GVL is lower than the LFL as a function of temperature is shown in fig. S9. For safe operation at 383 K, the reaction should be conducted above 3.6 bar oxygen pressure.

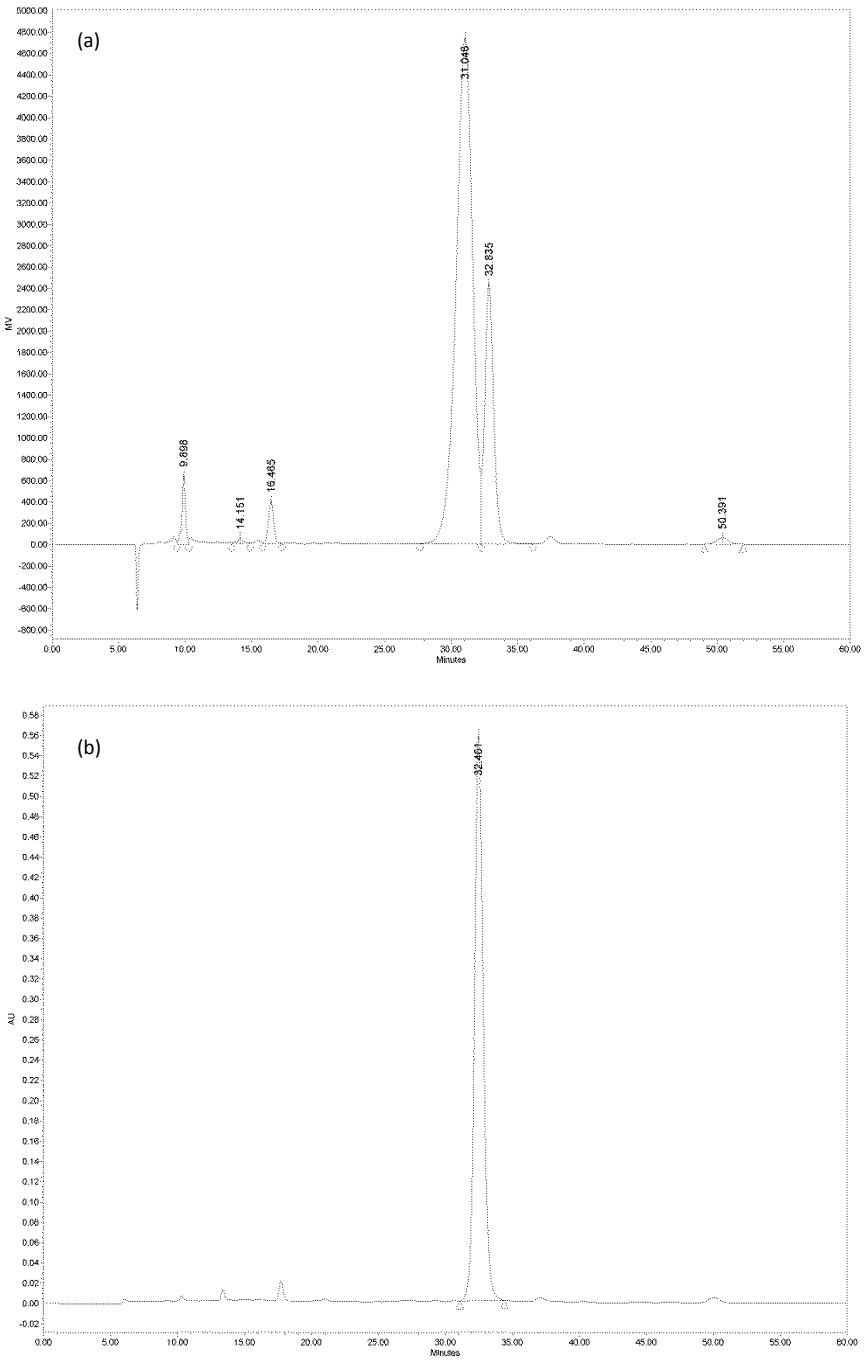


**fig. S1. Chromatogram of product solution obtained by the dehydration of fructose.** Reaction condition: Feed – 15 wt% Fructose; solvent – GVL:$H_2O$ = 50:50; reaction temperature – 453 K; acid concentration – 0.53 wt% FDCA; reaction time – 70 min. (**a**) Chromatogram using refractive index detector, fructose (9.9 min), formic acid (14.1 min), FDCA (16.4 min), GVL (31.0 min), HMF (32.8 min) and furfural (50.6 min). (**b**) Chromatogram using PDA detector (extracted at 320 nm); HMF (32.4 min).

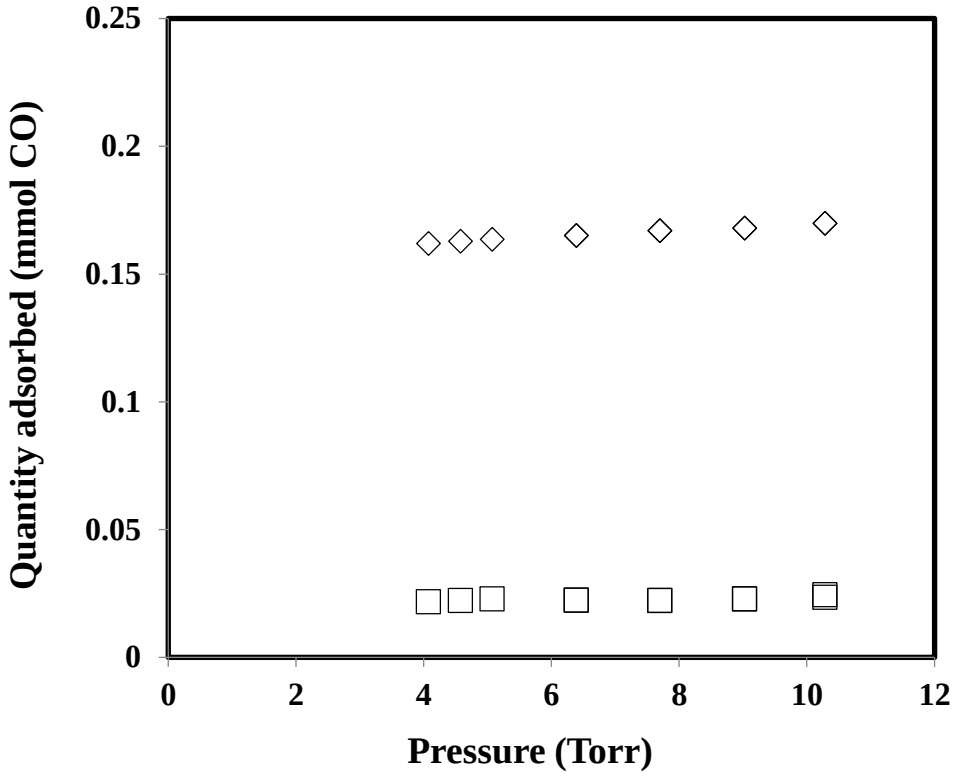


**fig. S2. CO chemisorption isotherms for the 5% Pt/C catalyst.** The reduced and passivated catalyst was re-reduced at 533 K in flowing $H_2$ and evacuated at 533 K for 1 hour. The first isotherm (□) was obtained at 308 K, after which the sample was evacuated at 308 K for 30 min, and then the second isotherm (□) was obtained at 308 K.

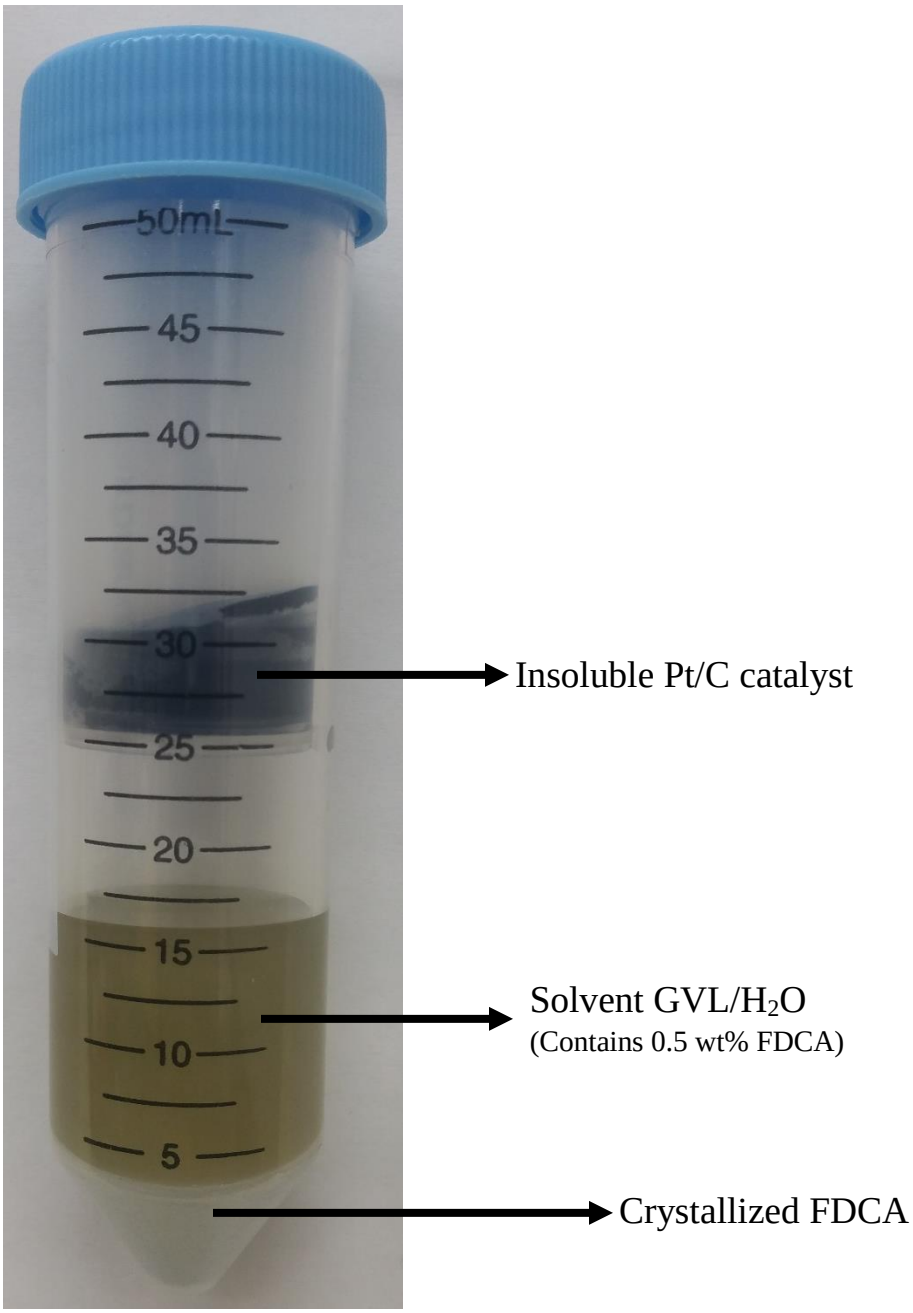


**fig. S3. Image showing the separation of catalyst, solvent, and crystallized FDCA.**
Separation was achieved using a centrifuge tube equipped with 0.2 um filter. After hot filtration the tube is cooled to 277 K leading to FDCA crystallization.

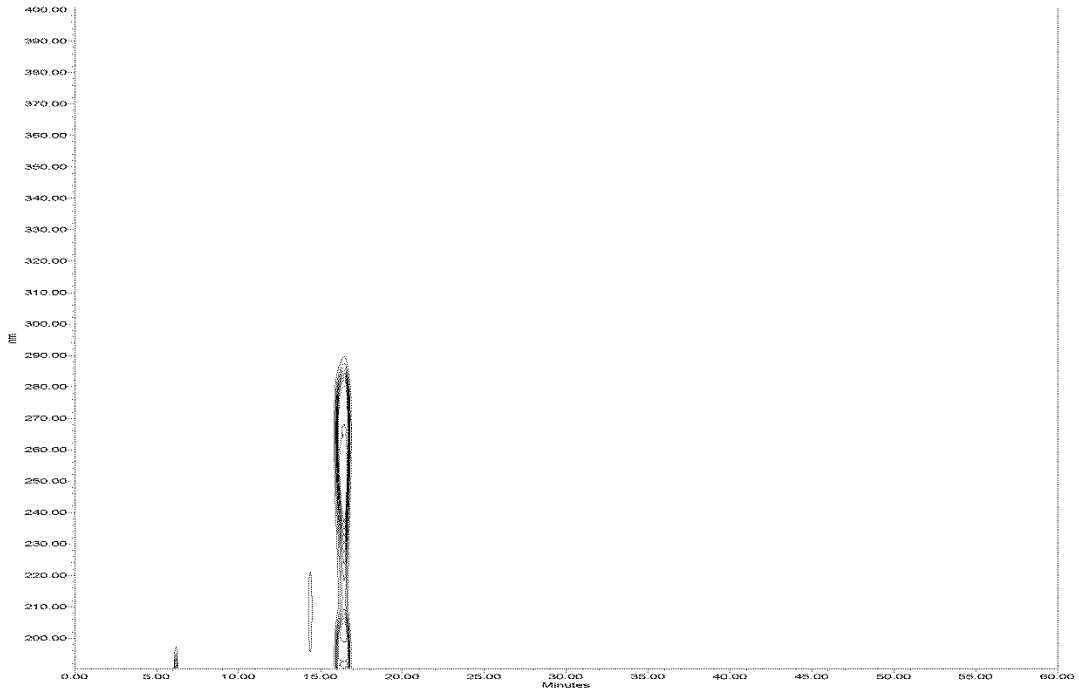


**fig. S4. PDA chromatogram of freeze-dried FDCA.** The FDCA peak is observed at 16.4 min.

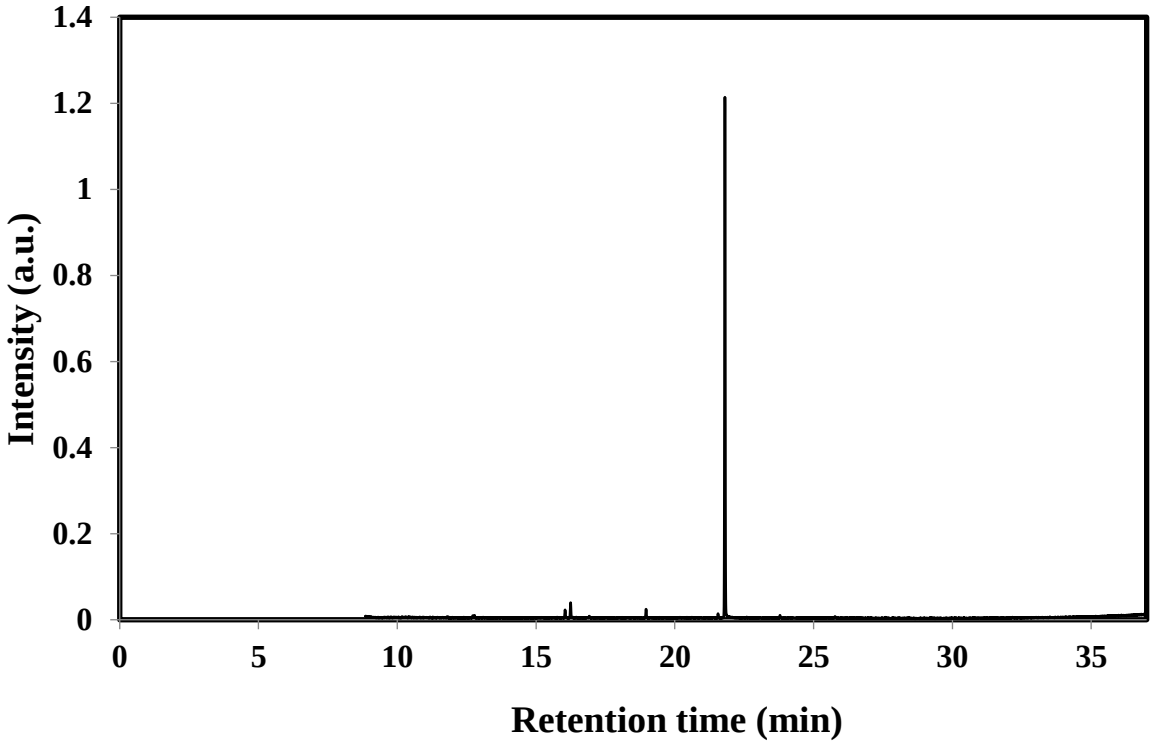


**fig. S5. Gas chromtography–mass spectrometry analysis of freeze-dried FDCA.** The FDCA retention time is 21.8 min. Small peaks at 16.3, 19.2, 21.6 and 24.0 min are due to bleeding from the silica column. The peak at 16.4 min is assigned to succinic acid (Butanedioic acid). The peak area for FDCA was 98.7% of the total peak area.

(a)

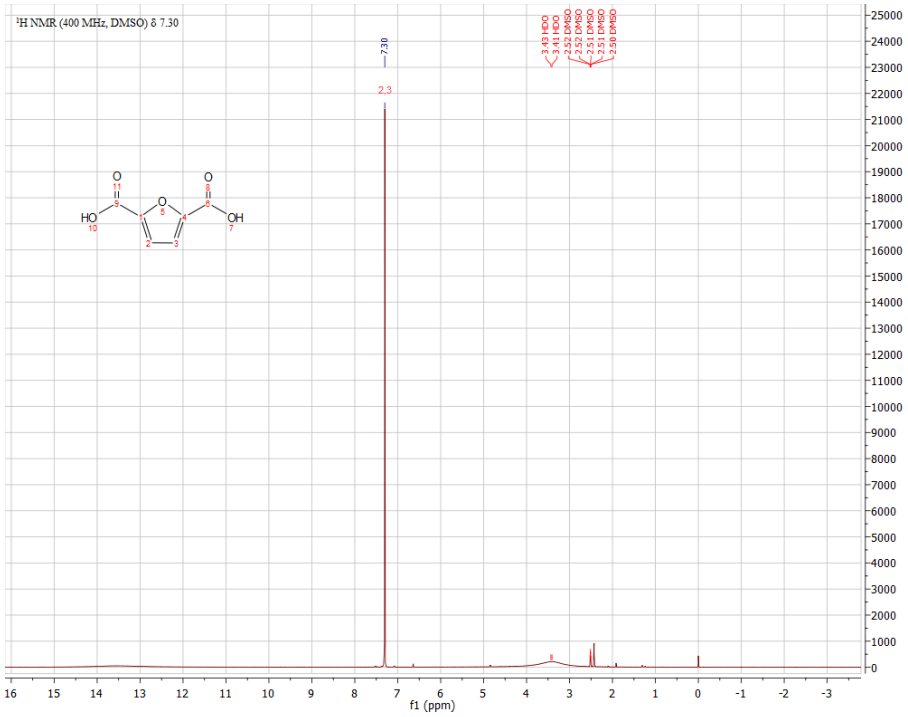


(b)

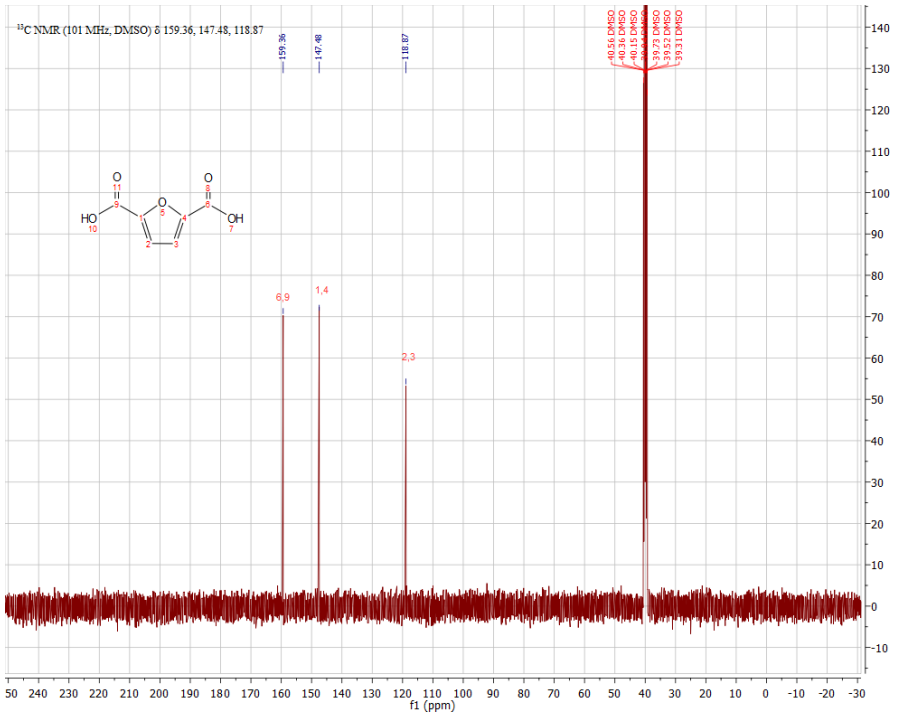


**fig. S6. Nuclear magnetic resonance spectroscopy analysis of freeze-dried FDCA.** (**a**) $^{1}H$ and (**b**) $^{13}C$ NMR of freeze-dried FDCA.

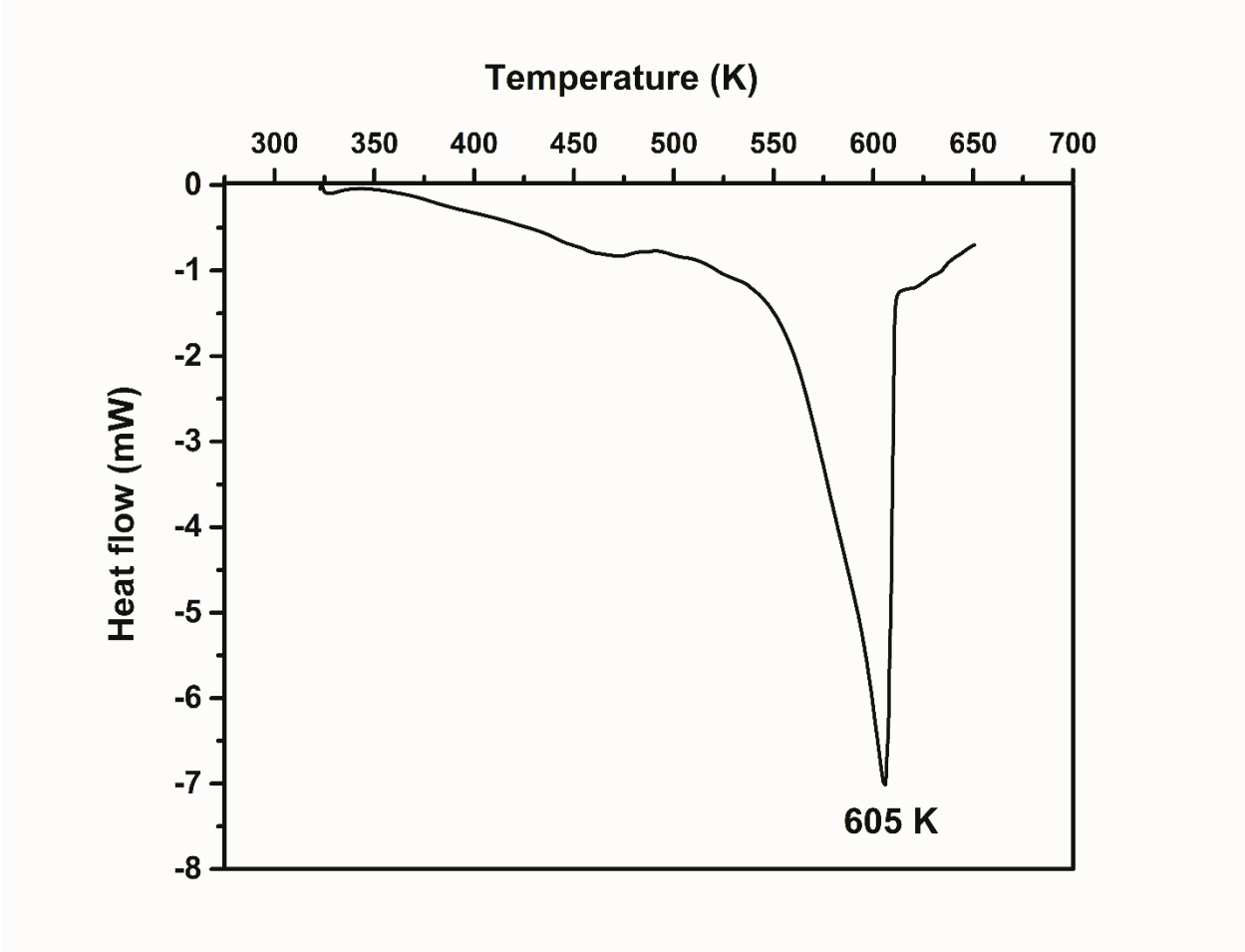


**fig. S7. Differential scanning calorimetry curve of freeze-dried FDCA.**

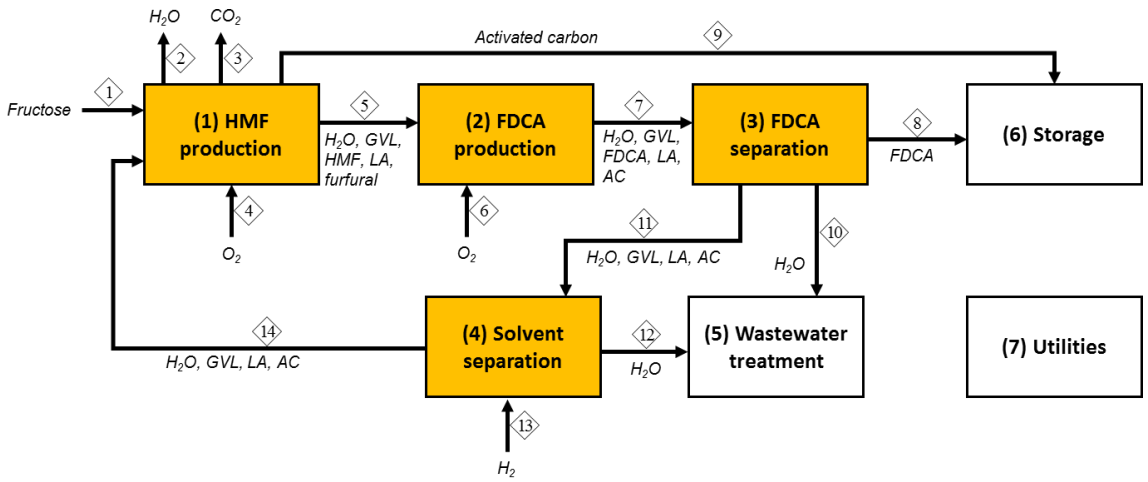


**fig. S8. Process block flow diagram for the integrated FDCA production strategy.** White sections are modified based on NREL's design (*29*) and yellow sections are developed based on the experimental data.

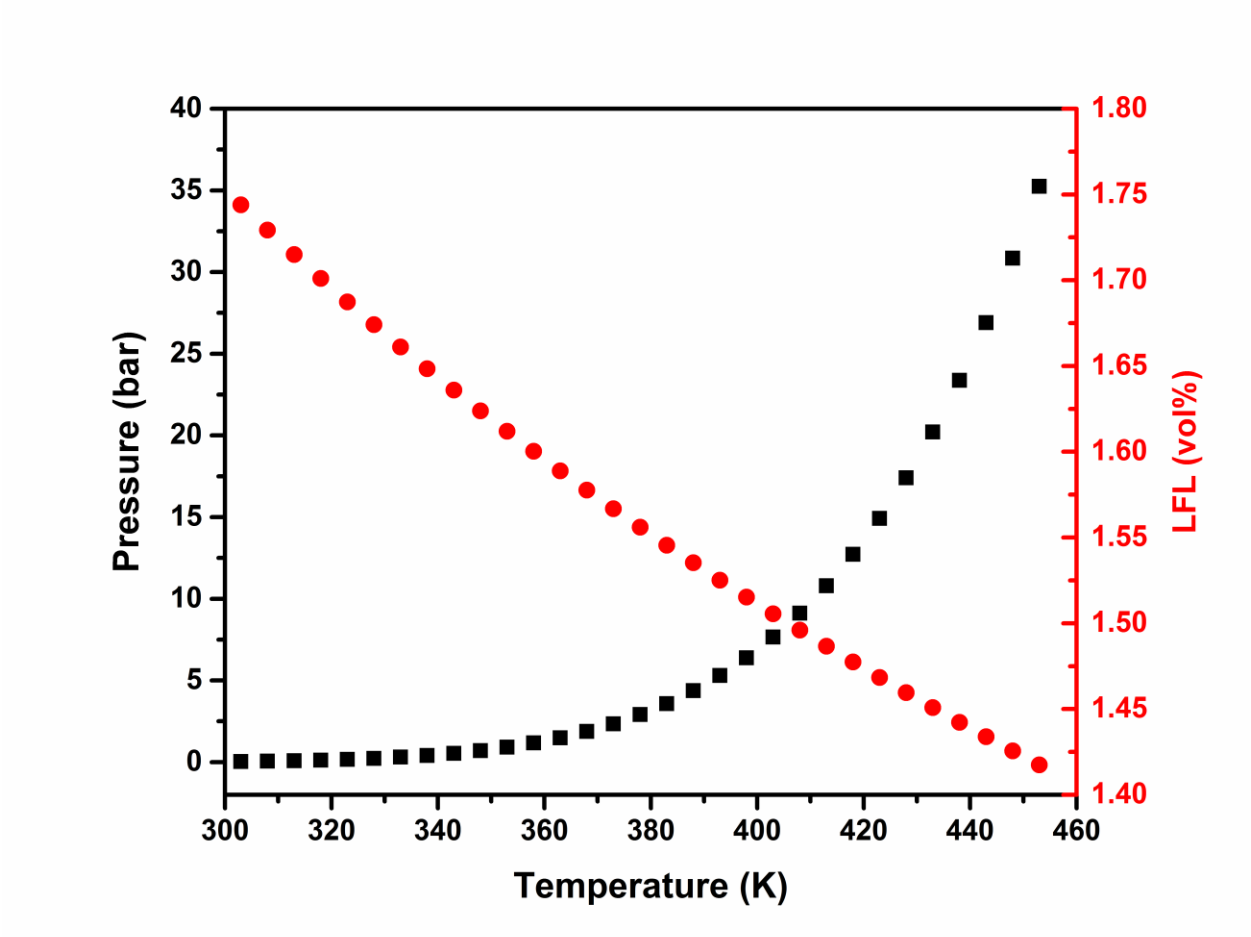


**fig. S9. Safety in the oxidation reactor.** Minimum pressure required to be below the lower flammability limit (LFL) of GVL as a function of temperature.

**table S1. Product composition after fructose dehydration using FDCA as a dehydration catalyst.**[a]

| Compound | Conversion/yield (%) |
|---|---|
| Fructose | 95.6 |
| HMF | 70.3 |
| Levulinic acid | 8.7 |
| Furfural | 3.1 |
| Unaccounted carbon | 13.5 |

[a] Reaction condition: Feed – 15 wt% Fructose; solvent – GVL:$H_2O$ = 50:50; reaction temperature – 453 K; acid concentration – 0.53 wt% FDCA; reaction time – 70 min.

**table S2. Product concentration before and after removal of humins by adsorption.**

| Compound | Concentration (M) | |
|---|---|---|
| | Before | After |
| Fructose | 0.05 | 0.05 |
| HMF | 0.58 | 0.57 |
| Levulinic acid | 0.07 | 0.06 |
| Furfural | 0.03 | 0.02 |

**table S3. Characterization of the Pt/C catalyst.**

| catalyst ID | Metal loading (ICP) | CO uptake ($\mu mol\ g^{-1}$) | dispersion (%) | average particle size (nm)* |
|---|---|---|---|---|
| Pt/C | 4.83 | 136 | 53 | 2.1 |

* Calculated by CO chemisorption: d(nm) = 110/Dispersion(%).

**table S4. Results for HMF oxidation reactions over the 5% Pt/C catalyst (under 40-bar $O_2$ pressure and 383 K).**

| # | HMF Concentration | Solvent (GVL:$H_2O$) | HMF: Pt | time (hours) | HMF conversion (%) | DFF Yield (%) | FFCA Yield (%) | FDCA Yield (%) |
|---|---|---|---|---|---|---|---|---|
| 1 | 7.5 wt% HMF + 3mM HCl | 50:50 | 30:1 | 16 | 100 | - | - | 5 |
| 2 | 7.5 wt% F-D HMF + ion exchange | 50:50 | 30:1 | 20 | 100 | - | - | 18 |

**table S5. Mass and energy balances (basis: 500 metric tons of fructose per day).**

| Major process section | Stream number | Mass flow (ton/h) | Pressure (atm) | Temperature (K) | Energy requirement (MW) |
|---|---|---|---|---|---|
| HMF production | 1 | 20.8 | 1 | 298 | Heating: 4.5<br>Electricity: 0.1 |
| | 2 | 3.0 | 20 | 873 | |
| | 3 | 4.2 | 20 | 873 | |
| | 4 | 3.0 | 1 | 298 | |
| | 9 | 1.7 | 20 | 873 | |
| | 14 | 124.1 | 20 | 378 | |
| FDCA production | 5 | 139.0 | 20 | 453 | Electricity: 0.1 |
| | 6 | 3.6 | 1 | 298 | |
| FDCA separation | 7 | 142.5 | 40 | 383 | Cooling: 18.9 |
| | 8 | 11.7 | 1 | 298 | |
| | 10 | 2.8 | 1 | 375 | |
| Solvent separation | 11 | 128.1 | 1 | 298 | Heating: 2.3<br>Cooling: 3.0<br>Electricity: 0.1 |
| | 12 | 4.0 | 1 | 373 | |
| | 13 | 0.003 | 1 | 298 | |

**table S6. Energy requirements (basis: 500 metric tons of fructose per day).**

| Energy required (MW) | Before heat integration | After heat integration |
|---|---|---|
| Heating | 41.1 | 6.9 |
| Cooling | 56.1 | 22.0 |

**table S7. Capital and operating costs (basis: 500 metric tons of fructose per day).**

| Process section | Capital cost ($10^6$$) | Operating cost ($10^6$$/yr) |
|---|---|---|
| HMF production[†,§] | 10.8 | 109.8 |
| FDCA production[†,§] | 16.4 | 12.7 |
| FDCA separation[†,§] | 4.9 | 0.5 |
| Solvent separation[§] | 1.2 | 0.9 |
| Wastewater treatment[†] | 6.0 | 0.3 |
| Storage[†] | 2.4 | 0.1 |
| Utilities[†] | 1.9 | 0.1 |
| Total installed equipment cost | 43.5 | |
| Total capital investment | 83.3 | |
| Total operating cost | | 124.4 |

Operating cost of each process section includes raw material cost (e.g., oxygen, hydrogen, and catalyst), utility cost (i.e., heating, cooling, and electricity), and fixed operating cost (e.g., salaries and property insurance).

[†] Estimated based on values reported in Davis et al. (*29*)

[§] Determined using Aspen Process Economic Analyzer (V8.8 Aspen Technology).

**table S8. List of economic parameters and assumptions.**

| | |
|---|---|
| Fructose price ($ per ton)[a] | 650.0 |
| Oxygen ($ per ton)[b] | 40.0 |
| Hydrogen ($ per ton)[c] | 1507.5 |
| Electricity ($ per kWh)[c] | 0.0572 |
| 5 wt% Pt/C ($ per kg)[d] | 194.0 |
| $RuSn_4$/C ($ per kg)[d] | 539.3 |
| Cooling tower chemicals ($ per ton)[c] | 3671.4 |
| Tax rate (%)[c] | 35.0 |

[a] Taken from Alibaba (*31*).

[b] Taken from Dorris et al. (*32*).

[c] Taken from Davis et al. (*29*).

[d] Taken from Han et al. (*33*).

Assumptions:

- 10% of the catalyst is refurbished every 6 months at a cost equivalent to 20% of its original value (*34*).
- Capital investment is spread over 3 years at a rate of 8%, 60%, and 32% in the first, second, and third years, respectively.
- Working capital is 5% of fixed capital investment.
- Discount rate is assumed to be 30%.
- Capital charge factor, calculated by discounted cash flow analysis, is 0.347.

**table S9. Effect of transport resistance and $O_2$ pressure on HMF oxidation over a Pt/C catalyst.[a]**

| # | Catalyst amount (g) | Liquid feed flow rate (ml/min) | Oxygen flow rate (ml/min) | Oxygen pressure (bar) | HMF conversion (%) | FFCA Yield (%) | FDCA Yield (%) |
|---|---|---|---|---|---|---|---|
| 1 | 0.5 | 0.02 | 25 | 40 | 100 | 27 | 69 |
| 2 | 1.0 | 0.04 | 50 | 40 | 100 | 17 | 74 |
| 3 | 1.0 | 0.04 | 50 | 20 | 100 | 21 | 71 |

[a]HMF oxidation over 5 wt% Pt/C. 1.0 wt% HMF in GVL:$H_2O$ (50:50) solution, temperature – 373 K